Journal of Thermal Science Vol.31, No.3 (2022) 712−726

https://doi.org/10.1007/s11630-022-1591-z **Article ID: 1003-2169(2022)03-0712-15**

A Model to Evaluate the Device-Level Performance of Thermoelectric Cooler with Thomson Effect Considered

GONG Tingrui[1,2*], GAO Lei[1,2], WU Yongjia[3], TAN Haoshu[1,2], QIN Feng[1,2], XIN Xiong[1,2], SHEN Limei[4], LI Juntao[1,2], MING Tingzhen[3]

1. Microsystem & Terahertz Research Center, China Academy of Engineering Physics, Chengdu 610200, China
2. Institute of Electronic Engineering, China Academy of Engineering Physics, Mianyang 621999, China
3. School of Civil Engineering and Architecture, Wuhan University of Technology, Wuhan 430070, China
4. Department of Refrigeration & Cryogenics Engineering, Huazhong University of Science and Technology, Wuhan 430074, China

Abstract: In this paper, a one-dimensional thermodynamic model was developed to evaluate the device-level performance of thermoelectric cooler (TEC) with the Thomson effect, contact resistance, gap heat leakage, heat sink, and heat load taken into account. The model was generalized and simplified by introducing dimensionless parameters. Experimental measurements showed good agreement with analytical results. The parametric analysis indicated that the influence of the Thomson effect on cooling capacity continued to expand with increasing current, while the effect on COP hardly changed with current. Low thermal contact resistance was beneficial to obtain lower hot-junction temperature, which can even reduce 2 K compared with the electrical contact resistance in the case study. The gap heat leakage was a negative factor affecting the cooling performance. When the thermal resistance of the heat sink was small, the negative effect of heat leakage on performance would be further enlarged. The enhancement of heat load temperature would increase the cooling power of the TEC. For example, an increase of 5 K in heat load can increase the cooling capacity by about 4%. However, once the current exceeded the optimum value, the raising effect on the cooling power would be weakened. The research can provide an analytical approach for the designer to perform trade studies to optimize the TEC system.

Keywords: thermoelectric cooler, thermodynamic model, Thomson effect, contact resistance, device-level performance

1. Introduction

Thermoelectric cooler (TEC) is a promising solid-state energy conversion technology that uses the Peltier effect for local heat dissipation. A typical TEC consists of multiple pairs of PN junctions. Each pair of PN junction is composed of two different doped semiconductor materials, one containing holes and the other electrons. When a current is applied, both types of charged carriers move away from the junction and convey heat way, thus cooling the cold junction. The absorbed heat is removed to the hot junction, where a heat exchanger is usually

Received: Apr 13, 2020 AE: QIU Lin Corresponding author: GONG Tingrui E-mail: trgonghust@163.com

Nomenclature

A	leg cross-sectional area/m^2
COP	coefficient of performance
E	electrical potential/V
I	electrical current/A
j	electrical current density/$A\cdot m^{-2}$
K	thermal conductance/$W\cdot K^{-1}$
K^*	dimensionless thermal conductance
k	thermal conductivity/$W\cdot m^{-1}\cdot K^{-1}$
L	leg length or leg height/m
n	n pairs of P, N-type thermoelements
P	input power/W
Q	heat flow rate/W
Q_c	heat absorption at cold-side/W
Q_h	heat rejection at hot-side/W
q	heat flux/$W\cdot m^{-2}$
R	electrical resistance/Ω
$R_{e,c1}$	electrical contact resistance of the thermoelement-solder interface/$\Omega\cdot m^2$
$R_{e,c2}$	electrical contact resistance of the Cu-solder interface/$\Omega\cdot m^2$
$R_{e,Cu}$	electrical resistance of copper connector/Ω
$R_{e,sol}$	electrical resistance of solder/Ω
$R_{k,c1}$	thermal contact resistance of the thermoelement-solder interface/$K\cdot m^2\cdot W^{-1}$
$R_{k,c2}$	thermal contact resistance of the Cu-solder interface/$K\cdot m^2\cdot W^{-1}$
$R_{k,Cu}$	thermal resistance of copper connector/$K\cdot W^{-1}$
$R_{k,G}$	thermal resistance of gap/$K\cdot W^{-1}$
$R_{k,hs}$	thermal resistance of heat sink/$K\cdot W^{-1}$
$R_{k,load}$	thermal resistance of heat load/$K\cdot W^{-1}$
$R_{k,sol}$	thermal resistance of solder/$K\cdot W^{-1}$
$R_{k,sub}$	thermal resistance of substrate/$K\cdot W^{-1}$
$R_{k,TIM}$	thermal resistance of TIM/$K\cdot W^{-1}$
T	temperature/K
ΔT	temperature difference, $\Delta T=T_h-T_c$ /K
x	displacement in the direction of leg length/m

Greek symbols

α	Seebeck coefficient/$V\cdot K^{-1}$
β	ratio of the Joule heat to the thermal conduction
β^*	reduced dimensionless parameter
γ	the ratio of the Joule heat to the thermal conduction
γ^*	reduced dimensionless parameter
Θ_c	dimensionless Peltier heat at the hot-junction of the thermoelement
Θ_h	dimensionless heat rejection at the hot-junction of the thermoelement
θ	dimensionless length
ξ	dimensionless length
Π_c	dimensionless Peltier heat at the cold-junction of the thermoelement
Π_h	dimensionless Peltier heat at the hot-junction of the thermoelement
ρ	electric resistivity/Ω·m
τ	thomson coefficient/$V\cdot K^{-1}$
ϕ	heat generation/$W\cdot m^{-3}$
Ψ	dimensionless power input

Subscripts

a	ambient
Cu	copper connector
gap	filling gap
H,C	hot, cold-end of the thermoelectric cooler
h,c	hot, cold-junction of the thermoelement
Load	heat load
P,N	P, N-type
sub	substrate
sol	solder
TE	thermoelement

placed to enhance the heat dissipation. Since TEC devices have the advantages of no moving parts, easy integration, precise temperature control, high reliability, and environmental friendliness, they have been widely used in microelectronic systems [1, 2], aerospace applications [3], medical equipment [4] and living environment [5]. According to different sizes and heat dissipating capacity, TEC can meet the different cooling needs of electronic devices due to its excellent local heat dissipation capacity. Nonetheless, how to establish an exact performance prediction model so that the TEC can be designed quickly and accurately according to the actual needs, has always been an important issue in the thermoelectric industry.

Generally, the design and performance evaluating of TEC devices are based on the mathematical modeling of thermoelectric phenomena in semiconductor materials. For many designs applied in practice, the ideal one-dimensional thermoelement model is widely used to model thermoelectric devices with complex multi-elements. It is assumed that the material properties, including the Seebeck coefficient, are constant and temperature-independent. Therefore, the Thomson effect, contact resistance, energy losses, and other parasitic losses are ignored in this model. As a result, these assumptions can lead to performance overestimation and even up to 10% error comparing to the true values [6].

Based on the ideal one-dimensional thermoelement model, many researchers have proposed various approaches to obtain the analytical relationship of the energy characteristics of thermoelectric devices from the completeness of mathematical description and the accuracy of the solution. Lee [7] formulated the classical basic equations for a typical TEC and derived the exact solutions to study the Thomson effect in conjunction with the ideal equation. It was found that the positive Thomson coefficient slightly improved the performance of a TEC while the negative Thomson coefficient slightly reduced the performance. Indeed, the Thomson effect affects 5%–7% of the performance of thermoelectric devices, and it still plays a substantial role in obtaining exact solutions and optimal performance [8, 9]. If the Thomson effect can be fully utilized, it would be possible to significantly increase the performance of the TEC. For example, Snyder et al. [10] proposed a Thomson cooler, which required an exponentially rising Seebeck coefficient with increasing temperature. Under reasonable conditions, the maximum temperature drop of the Thomson cooler is predicted to be twice that of the conventional Peltier cooler. Zhou et al. [11] established a mathematical model for the novel combined cross-regenerative cross flow (C-RC) thermoelectric-assisted indirect evaporative cooling (TIEC) system, and performed system performance analysis and optimization. The results showed that the C-RC TIEC system had a superior COP, especially when the number of thermoelectric cooling modules and working current were small.

Since thermoelectric devices are assembled by stacking different material layers, the resulting interface contact resistances inevitably yield higher thermal and electrical losses and finally degrade the device performance. The impacts of the losses caused by contact resistances on the performance of thermoelectric devices have received more and more attention. Min et al. [12] suggested that both COP and heat pumping capacity can achieve further improvement by reducing the contact resistances, especially the thermal contact resistance. Jeong [13] proposed a novel one-dimensional analytical model and found that the increase in contact resistance would significantly reduce the maximum COP. In addition, when the thermoelectric devices are reduced to micro-scale, the practical cooling performance of the TEC is severely limited by contact resistance [14, 15]. Sun et al. [16] developed an effective method for evaluating the cooling performance of micro TEC with interfacial and size effects considered. Both the boundary and size effects were found to weaken the cooling performance of the TEC at the device level. Qiu et al. [17] presented a comprehensive study of TEC with non-constant and constant cross sections. The results showed that different contact layers had different sensitivity to cooling performance.

Moreover, thermoelectric devices are often used as subsystems of complex systems, including heat mediums, heat sinks, multilayer thermal and electrical insulators, interconnects and controllers, etc. [18]. Unlike standalone thermoelectric modules, device consideration requires a holistic approach. Wang et al. [19] developed a generalized analytical model for the optimization of a TEC system by introducing the entropy generation analysis method. Wu et al. [20] proposed an accurate thermodynamic model and analyzed the device-level performance of a thermoelectric device considering the influences of the contact layer resistance, Thomson effect, heat sink, and thermo-pellet gap heat leakage. Melnikov et al. [21] proposed a dimensionless mathematical model of TEC, taking into account thermal resistance between the thermoelectric material and the heat source. Zhang [22] developed a analytical approach to evaluate and optimize TEC system based on the TEC thermal balance equations. Performance parameters such as cooling power and device temperature at both the TE pellet level and module level were presented in simplified formulation. Cai et al. [23] established an analytical model of a thermoelectric micro cooler based on the method of effectiveness-number of transfer units. The effects of thermoelectric properties and the scale of the extender block on cooling performance were studied. Pearson et al. [24] quantified the possible benefits of a TEC implemented within a thermal resistance network in the thermal system. Zhou et al. [25] presented a theoretical model of a TEC system with the thermal conductances from the hot and cold sides taken into account. Lu et al. [26] developed an integrated theoretical and experimental method to study the thermal resistance matching for real thermoelectric cooling systems, including hot and cold side heat sinks and the thermoelectric modules. Tan et al. [27] presented an analytical model based on the second law of thermodynamics to study the optimal performance of a thermoelectric cooling system. Gonzalez-Hernandez [28]

presented an energy analysis for a thermoelectric system operated as cooler and as heat pump TEC and thermoelectric heater. Guo et al. [29] proposed a two-stage thermoelectric generator as the waste heat recovery technology for a high-temperature proton exchange membrane fuel cell. The energetic and exergetic performances of the hybrid system were investigated.

Based on the above literature review, the known researches still present the following imperfections: the complexity of analytical methods and the laboriousness of the calculations, the lack of considerate impact factors to accurately deliver to practical application, the lack of simplicity for engineering applications, and the insufficient validity. As a result, there arises the problem of developing a sophisticated model with sufficient accuracy to predict the device-level performance of TEC without some unnecessary assumptions. In this paper, a new one-dimensional thermodynamic model was developed to evaluate the device-level performance. The model was generalized and simplified by introducing dimensionless parameters, which can be used to predict the cooling performance of various TEC devices. The model was validated by the experimental results of commercial TEC devices. The influences of the Thomson effect, contact resistance, gaps heat leakage, heat load and heat sink on the cooling performance were investigated. The thermodynamic model proposed in this study avoids some unnecessary simplifications and provides an analytical approach for the designer to perform trade studies to optimize the TEC system.

2. Thermodynamic Model

Fig. 1(a) shows a schematic diagram of a realistic single thermocouple, which is the basic unit of a TEC device. A P-type thermoelement and an N-type thermoelement were connected electrically in series and thermally in parallel by solders and Cu connectors. Ceramic substrates were attached on both sides of the thermoelements to isolate the thermocouple electrically. In practical applications, the cold end of the TEC was typically brought into contact with the heat load. The heat generated by the heat load was pumped to the hot end of the TEC via the Peltier effect. After that, the heat was dissipated into the ambient through a heat sink. Thermal interface material (TIM) with low thermal resistance was assumed to provide good thermal

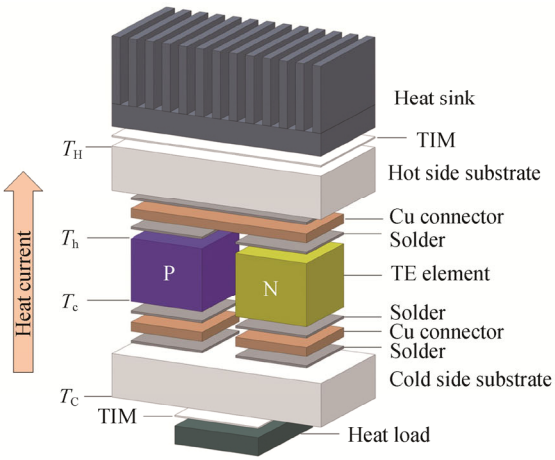

(a) A realistic single thermocouple of the TEC device

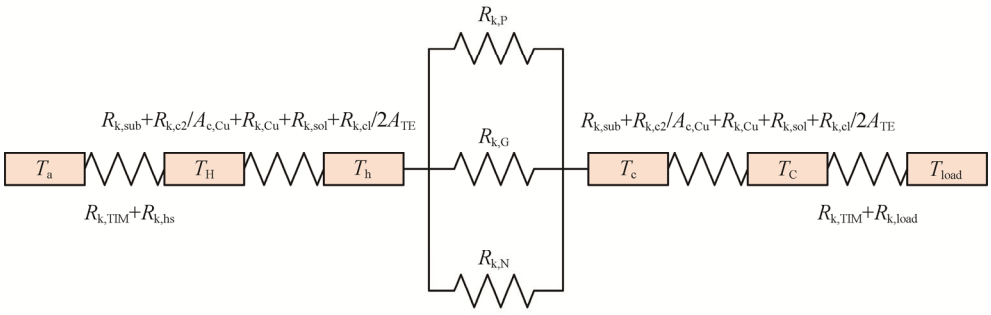

(b) Thermal network

Fig. 1 Schematic diagram of (a) a realistic single thermocouple of the TEC device and (b) thermal network

connections at the contact interfaces. The heat current from the heat load to the heat sink was defined to be positive, as shown in Fig. 1(a). T_h and T_c were the hot side temperature and the cold side temperature of the thermoelement. T_H and T_C denoted the temperature at the hot side substrate and that at the cold side substrate. Due to the thermal contact resistances of material layers, T_c will be lower than $T_{C,}$ and T_h will be higher than T_H in a stable thermal equilibrium condition. The additional thermal resistances due to heat load, heat sink, contact resistance, and gap thermal leakage were connected in series or parallel to the thermocouple's thermal network, as shown in Fig. 1(b). The simple and rather accurate analytical model thus can be deduced for evaluating the device-level performance under the minimum amount of simplifying assumptions.

Considering a non-uniformly heated thermoelectric material with isotropic material properties, the electrical current conservation equation in one-dimensional thermoelement is given as:

$$\frac{\mathrm{d}j}{\mathrm{d}x}=0 \tag{1}$$

The electric field is given by a combination of the reversible Seebeck effect and the irreversible Joule effect. Combining the Seebeck and Joule effects, the electric field is given as:

$$E=j\rho+\alpha\frac{\mathrm{d}T}{\mathrm{d}x} \tag{2}$$

Similarly, heat is transported reversibly by the Peltier effect, and irreversibly by the Fourier's law that is also affected by the Joule effect. Thus the heat flux is given by:

$$q=\alpha Tj-k\frac{\mathrm{d}T}{\mathrm{d}x} \tag{3}$$

The general heat transfer equation for steady-state is:

$$-\frac{\mathrm{d}q}{\mathrm{d}x}+\phi=0 \tag{4}$$

where ϕ is expressed by:

$$\phi=E\cdot j=j^2\rho+j\cdot\alpha\frac{\mathrm{d}T}{\mathrm{d}x} \tag{5}$$

Then the steady-state thermal energy transport equation is governed by [6, 7]:

$$\frac{\mathrm{d}}{\mathrm{d}x}\cdot\left(k\frac{\mathrm{d}T}{\mathrm{d}x}\right)+j^2\rho-T\frac{\mathrm{d}\alpha}{\mathrm{d}T}j\cdot\frac{\mathrm{d}T}{\mathrm{d}x}=0 \tag{6}$$

where α is the Seebeck coefficient; T is the temperature; ρ is the electric resistivity; k is the thermal conductivity; and j is the electrical current density flow. The first term describes the thermal conduction; the second term represents the Joule heat, and the third term is the Thomson heat.

The Thomson coefficient is defined by:

$$\tau=T\frac{\mathrm{d}\alpha}{\mathrm{d}T} \tag{7}$$

For moderate temperature differences, the Thomson coefficient can be assumed a constant without causing much deviation. Besides, the combined radiation and convection heat transfer rate with ambient can be negligible due to the small temperature difference and the small exposed surface area of the thermoelements [9, 30].

Generally, P, N-type thermoelement correspond to different material properties. The thermodynamic control equations in one-dimensional thermoelements can be written as:

$$\mathrm{P}:\ \frac{\mathrm{d}^2T}{\mathrm{d}x^2}-\frac{I\tau_\mathrm{P}}{k_\mathrm{P}A_\mathrm{P}}\frac{\mathrm{d}T}{\mathrm{d}x}+\frac{I^2\rho_\mathrm{P}}{k_\mathrm{P}A_\mathrm{P}^2}=0 \tag{8}$$

$$\mathrm{N}:\ \frac{\mathrm{d}^2T}{\mathrm{d}x^2}+\frac{I\tau_\mathrm{N}}{k_\mathrm{N}A_\mathrm{N}}\frac{\mathrm{d}T}{\mathrm{d}x}+\frac{I^2\rho_\mathrm{N}}{k_\mathrm{N}A_\mathrm{N}^2}=0 \tag{9}$$

In Eqs. (8) and (9), the boundary conditions refer to be $T(0)=T_c$ and $T(L)=T_h$.

The dimensionless parameters can reduce the number of independent parameters, thus offer convenience to generalize and simplify the shape of the governing equations as:

$$\mathrm{P}:\ \frac{\mathrm{d}^2\theta}{\mathrm{d}\xi^2}-\beta_\mathrm{P}\frac{\mathrm{d}\theta}{\mathrm{d}\xi}+\gamma_\mathrm{P}=0 \tag{10}$$

$$\mathrm{N}:\ \frac{\mathrm{d}^2\theta}{\mathrm{d}\xi^2}+\beta_\mathrm{N}\frac{\mathrm{d}\theta}{\mathrm{d}\xi}+\gamma_\mathrm{N}=0 \tag{11}$$

The corresponding boundary conditions can be written as:

$$\theta=\frac{T-T_c}{T_h-T_c}\ \text{ and }\ \xi=\frac{x}{L} \tag{12}$$

where $\theta(0)=0$ and $\theta(L)=1$.

$$\beta_\mathrm{P}=\frac{I\tau_\mathrm{P}\Delta T}{k_\mathrm{P}A_\mathrm{P}\dfrac{\Delta T}{L_\mathrm{P}}},\ \ \beta_\mathrm{N}=\frac{I\tau_\mathrm{N}\Delta T}{k_\mathrm{N}A_\mathrm{N}\dfrac{\Delta T}{L_\mathrm{N}}} \tag{13}$$

where β is the ratio of the Thomson heat to the thermal conduction.

$$\gamma_\mathrm{P}=\frac{I^2R_\mathrm{P}}{k_\mathrm{P}A_\mathrm{P}\dfrac{\Delta T}{L_\mathrm{P}}},\ \ \gamma_\mathrm{N}=\frac{I^2R_\mathrm{N}}{k_\mathrm{N}A_\mathrm{N}\dfrac{\Delta T}{L_\mathrm{N}}} \tag{14}$$

where γ is the ratio of the Joule heat to the thermal conduction. The electrical resistances of P, N-type thermoelements are:

$$R_\mathrm{P}=\frac{\rho_\mathrm{P}L_\mathrm{P}}{A_\mathrm{P}},\ \ R_\mathrm{N}=\frac{\rho_\mathrm{N}L_\mathrm{N}}{A_\mathrm{N}} \tag{15}$$

The thermal conductance of P, N-type thermoelement are given by:

$$K_\mathrm{P}=\frac{k_\mathrm{P}A_\mathrm{P}}{L_\mathrm{P}},\ \ K_\mathrm{N}=\frac{k_\mathrm{N}A_\mathrm{N}}{L_\mathrm{N}} \tag{16}$$

The temperature difference is:

$$\Delta T=T_h-T_c \tag{17}$$

where T_h and T_c are the temperatures of the hot and cold junctions of the thermoelement, respectively.

Solving the equation above, the temperature profiles in the P, N-type thermoelement are described as follows:

$$\mathrm{P}:\ \theta(\xi)=\frac{\beta_{\mathrm{P}}-\gamma_{\mathrm{P}}}{\left(e^{\beta_{\mathrm{P}}}-1\right)\beta_{\mathrm{P}}}\left(e^{\beta_{\mathrm{P}}\xi}-1\right)+\frac{\gamma_{\mathrm{P}}}{\beta_{\mathrm{P}}}\xi \tag{18}$$

$$\mathrm{N}:\ \theta(\xi)=\frac{\beta_{\mathrm{N}}+\gamma_{\mathrm{N}}}{\left(1-e^{-\beta_{\mathrm{N}}}\right)\beta_{\mathrm{N}}}\left(1-e^{-\beta_{\mathrm{N}}\xi}\right)-\frac{\gamma_{\mathrm{N}}}{\beta_{\mathrm{N}}}\xi \tag{19}$$

Heat flux in the cross-section can be calculated by:

$$Q=\alpha TI+kA\frac{\mathrm{d}T}{\mathrm{d}x} \tag{20}$$

According to the principle of energy balance, the heat flux in the hot, cold-junction is given as:

$$\begin{aligned}Q_{\mathrm{h}}&=Q_{\mathrm{P,h}}+Q_{\mathrm{N,h}}\\&=\left(\alpha_{\mathrm{P,h}}-\alpha_{\mathrm{N,h}}\right)T_{\mathrm{h}}I-k_{\mathrm{P}}A_{\mathrm{P}}\left.\frac{\mathrm{d}T}{\mathrm{d}x}\right|_{x=L_{\mathrm{P}}}-k_{\mathrm{N}}A_{\mathrm{N}}\left.\frac{\mathrm{d}T}{\mathrm{d}x}\right|_{x=L_{\mathrm{N}}}\end{aligned} \tag{21}$$

$$\begin{aligned}Q_{\mathrm{c}}&=Q_{\mathrm{P,c}}+Q_{\mathrm{N,c}}\\&=\left(\alpha_{\mathrm{P,c}}-\alpha_{\mathrm{N,c}}\right)T_{\mathrm{c}}I-k_{\mathrm{P}}A_{\mathrm{P}}\left.\frac{\mathrm{d}T}{\mathrm{d}x}\right|_{x=0}-k_{\mathrm{N}}A_{\mathrm{N}}\left.\frac{\mathrm{d}T}{\mathrm{d}x}\right|_{x=0}\end{aligned} \tag{22}$$

Correspondingly, the dimensionless cooling power is expressed as:

$$\begin{aligned}\Theta_{\mathrm{h}}&=\Theta_{\mathrm{P,h}}+\Theta_{\mathrm{N,h}}=\frac{Q_{\mathrm{P,h}}+Q_{\mathrm{N,h}}}{k_{\mathrm{P}}A_{\mathrm{P}}\Delta T/L_{\mathrm{P}}+k_{\mathrm{N}}A_{\mathrm{N}}\Delta T/L_{\mathrm{N}}}\\&=\Pi_{\mathrm{h}}-\frac{k_{\mathrm{P}}A_{\mathrm{P}}\Delta T/L_{\mathrm{P}}}{k_{\mathrm{P}}A_{\mathrm{P}}\Delta T/L_{\mathrm{P}}+k_{\mathrm{N}}A_{\mathrm{N}}\Delta T/L_{\mathrm{N}}}\left.\frac{\mathrm{d}\theta_{\mathrm{P}}}{\mathrm{d}\xi}\right|_{\xi=1}\\&\quad-\frac{k_{\mathrm{N}}A_{\mathrm{N}}\Delta T/L_{\mathrm{N}}}{k_{\mathrm{P}}A_{\mathrm{P}}\Delta T/L_{\mathrm{P}}+k_{\mathrm{N}}A_{\mathrm{N}}\Delta T/L_{\mathrm{N}}}\left.\frac{\mathrm{d}\theta_{\mathrm{N}}}{\mathrm{d}\xi}\right|_{\xi=1}\end{aligned} \tag{23}$$

$$\begin{aligned}\Theta_{\mathrm{c}}&=\Theta_{\mathrm{P,c}}+\Theta_{\mathrm{N,c}}=\frac{Q_{\mathrm{P,c}}+Q_{\mathrm{N,c}}}{k_{\mathrm{P}}A_{\mathrm{P}}\Delta T/L_{\mathrm{P}}+k_{\mathrm{N}}A_{\mathrm{N}}\Delta T/L_{\mathrm{N}}}\\&=\Pi_{\mathrm{c}}-\frac{k_{\mathrm{P}}A_{\mathrm{P}}\Delta T/L_{\mathrm{P}}}{k_{\mathrm{P}}A_{\mathrm{P}}\Delta T/L_{\mathrm{P}}+k_{\mathrm{N}}A_{\mathrm{N}}\Delta T/L_{\mathrm{N}}}\left.\frac{\mathrm{d}\theta_{\mathrm{P}}}{\mathrm{d}\xi}\right|_{\xi=0}\\&\quad-\frac{k_{\mathrm{N}}A_{\mathrm{N}}\Delta T/L_{\mathrm{N}}}{k_{\mathrm{P}}A_{\mathrm{P}}\Delta T/L_{\mathrm{P}}+k_{\mathrm{N}}A_{\mathrm{N}}\Delta T/L_{\mathrm{N}}}\left.\frac{\mathrm{d}\theta_{\mathrm{N}}}{\mathrm{d}\xi}\right|_{\xi=0}\end{aligned} \tag{24}$$

And the dimensionless Peltier heat is defined as:

$$\Pi_{\mathrm{h}}=\frac{\alpha_{\mathrm{P,h}}T_{\mathrm{h}}I-\alpha_{\mathrm{N,h}}T_{\mathrm{h}}I}{k_{\mathrm{P}}A_{\mathrm{P}}\Delta T/L_{\mathrm{P}}+k_{\mathrm{N}}A_{\mathrm{N}}\Delta T/L_{\mathrm{N}}} \tag{25}$$

$$\Pi_{\mathrm{c}}=\frac{\alpha_{\mathrm{P,c}}T_{\mathrm{c}}I-\alpha_{\mathrm{N,c}}T_{\mathrm{c}}I}{k_{\mathrm{P}}A_{\mathrm{P}}\Delta T/L_{\mathrm{P}}+k_{\mathrm{N}}A_{\mathrm{N}}\Delta T/L_{\mathrm{N}}} \tag{26}$$

Thus the dimensionless heat flux in the hot/cold junction of the thermoelement can be given by:

$$\begin{aligned}\Theta_{\mathrm{h}}&=\Pi_{\mathrm{h}}-\left[\left(K_{\mathrm{P}}^{*}\beta_{\mathrm{P}}^{*}+K_{\mathrm{N}}^{*}\beta_{\mathrm{N}}^{*}\right)+\left(K_{\mathrm{P}}^{*}\beta_{\mathrm{P}}-K_{\mathrm{N}}^{*}\beta_{\mathrm{N}}\right)\right]\\&\quad-\left[\left(K_{\mathrm{P}}^{*}\gamma_{\mathrm{P}}^{*}+K_{\mathrm{N}}^{*}\gamma_{\mathrm{N}}^{*}\right)-\left(K_{\mathrm{P}}^{*}\gamma_{\mathrm{P}}+K_{\mathrm{N}}^{*}\gamma_{\mathrm{N}}\right)\right]\end{aligned} \tag{27}$$

$$\Theta_{\mathrm{c}}=\Pi_{\mathrm{c}}-\left(K_{\mathrm{P}}^{*}\beta_{\mathrm{P}}^{*}+K_{\mathrm{N}}^{*}\beta_{\mathrm{N}}^{*}\right)-\left(K_{\mathrm{P}}^{*}\gamma_{\mathrm{P}}^{*}+K_{\mathrm{N}}^{*}\gamma_{\mathrm{N}}^{*}\right) \tag{28}$$

where:

$$\begin{aligned}K_{\mathrm{P}}^{*}&=\frac{k_{\mathrm{P}}A_{\mathrm{P}}\Delta T/L_{\mathrm{P}}}{k_{\mathrm{N}}A_{\mathrm{N}}\Delta T/L_{\mathrm{N}}+k_{\mathrm{P}}A_{\mathrm{P}}\Delta T/L_{\mathrm{P}}}\\K_{\mathrm{N}}^{*}&=\frac{k_{\mathrm{N}}A_{\mathrm{N}}\Delta T/L_{\mathrm{N}}}{k_{\mathrm{N}}A_{\mathrm{N}}\Delta T/L_{\mathrm{N}}+k_{\mathrm{P}}A_{\mathrm{P}}\Delta T/L_{\mathrm{P}}}\end{aligned} \tag{29}$$

$$\beta_{\mathrm{P}}^{*}=\frac{\beta_{\mathrm{P}}}{e^{\beta_{\mathrm{P}}}-1},\quad \beta_{\mathrm{N}}^{*}=\frac{\beta_{\mathrm{N}}}{1-e^{-\beta_{\mathrm{N}}}} \tag{30}$$

$$\gamma_{\mathrm{P}}^{*}=\gamma_{\mathrm{P}}\left(\frac{1}{\beta_{\mathrm{P}}}-\frac{1}{e^{\beta_{\mathrm{P}}}-1}\right),\quad \gamma_{\mathrm{N}}^{*}=\gamma_{\mathrm{N}}\left(\frac{1}{1-e^{-\beta_{\mathrm{N}}}}-\frac{1}{\beta_{\mathrm{N}}}\right) \tag{31}$$

In Eqs. (27) and (28), the first term describes the Peltier cooling; the second term specifies the Thompson heat, and the third term explains the Joule heat. Θ_{h} and Θ_{c} are the dimensionless heat rejection at the hot-junction of the thermoelement and the dimensionless heat absorption at the cold-junction of the thermoelement, respectively.

Then the dimensionless power input of the model is given by:

$$\begin{aligned}\Psi&=\Theta_{\mathrm{h}}-\Theta_{\mathrm{c}}=\left(\Pi_{\mathrm{h}}-\Pi_{\mathrm{c}}\right)\\&\quad+\left(K_{\mathrm{N}}^{*}\beta_{\mathrm{N}}-K_{\mathrm{P}}^{*}\beta_{\mathrm{P}}\right)+\left(K_{\mathrm{P}}^{*}\gamma_{\mathrm{P}}+K_{\mathrm{N}}^{*}\gamma_{\mathrm{N}}\right)\end{aligned} \tag{32}$$

Since a TEC consists of n pairs of thermoelements, it is possible to use the thermoelement cooling capacity in Eq. (22) or Eq. (28) to multiply with thermoelement numbers to obtain the TEC cooling capacity [31]. Likewise, the coefficient of performance (COP) of a TEC with n pairs of P, N-type thermoelement is determined as follows:

$$\begin{aligned}\mathrm{COP}&=\frac{n\Theta_{\mathrm{c}}}{n\Psi}\\&=\frac{\Pi_{\mathrm{c}}-\left(K_{\mathrm{P}}^{*}\beta_{\mathrm{P}}^{*}+K_{\mathrm{N}}^{*}\beta_{\mathrm{N}}^{*}\right)-\left(K_{\mathrm{P}}^{*}\gamma_{\mathrm{P}}^{*}+K_{\mathrm{N}}^{*}\gamma_{\mathrm{N}}^{*}\right)}{\left(\Pi_{\mathrm{h}}-\Pi_{\mathrm{c}}\right)+\left(K_{\mathrm{N}}^{*}\beta_{\mathrm{N}}-K_{\mathrm{P}}^{*}\beta_{\mathrm{P}}\right)+\left(K_{\mathrm{P}}^{*}\gamma_{\mathrm{P}}+K_{\mathrm{N}}^{*}\gamma_{\mathrm{N}}\right)}\end{aligned} \tag{33}$$

The present model is still applicable and effective when the geometry and material properties are changed.

In a real TEC module, the gaps between the TE elements are filled with electrical insulation material to reduce the thermal stress and heat leakage in the module. Since the operating temperature of the TEC is not high, the radiant heat loss is generally negligible. Besides, since the gaps are filled with the insulating material, the convective heat loss is negligible. Therefore, the thermal conductance through the gap can be expressed as:

$$K_{\mathrm{gap}}=\frac{k_{\mathrm{gap}}A_{\mathrm{gap}}}{L_{\mathrm{gap}}} \tag{34}$$

In the thermally stable state, the heat flow at the hot-junction of the thermoelement would return to the cold-junction through the gap. Then the heat flow can be expressed as:

$$Q_{\mathrm{gap}}=K_{\mathrm{gap}}\left(T_{\mathrm{h}}-T_{\mathrm{c}}\right) \tag{35}$$

The thermal resistance of the substrate, copper

connector and solder are given by:

$$R_{\mathrm{k,sub}}=\frac{L_{\mathrm{sub}}}{k_{\mathrm{sub}}A_{\mathrm{sub}}} \tag{36}$$

$$R_{\mathrm{k,Cu}}=\frac{L_{\mathrm{Cu}}}{k_{\mathrm{Cu}}A_{\mathrm{Cu}}} \tag{37}$$

$$R_{\mathrm{k,sol}}=\frac{L_{\mathrm{sol}}}{k_{\mathrm{sol}}A_{\mathrm{sol}}} \tag{38}$$

The energy conservation equation in the hot and cold end can be expressed as:

$$\begin{aligned}Q_{\mathrm{C}}&=\frac{T_{\mathrm{C}}-T_{\mathrm{c}}}{R_{\mathrm{k,sub}}+\dfrac{R_{\mathrm{k,c2}}}{A_{\mathrm{Cu}}}+R_{\mathrm{k,Cu}}+R_{\mathrm{k,sol}}+\dfrac{R_{\mathrm{k,c1}}}{2A_{\mathrm{TE}}}}\\&=Q_{\mathrm{c}}-Q_{\mathrm{gap}}-I^2R_{\mathrm{e,Cu}}-I^2R_{\mathrm{e,sol}}-2I^2\frac{R_{\mathrm{e,c1}}+R_{\mathrm{e,c2}}}{A_{\mathrm{TE}}}\end{aligned} \tag{39}$$

$$\begin{aligned}Q_{\mathrm{H}}&=\frac{T_{\mathrm{h}}-T_{\mathrm{H}}}{R_{\mathrm{k,sub}}+\dfrac{R_{\mathrm{k,c2}}}{A_{\mathrm{Cu}}}+R_{\mathrm{k,Cu}}+R_{\mathrm{k,sol}}+\dfrac{R_{\mathrm{k,c1}}}{2A_{\mathrm{TE}}}}\\&=Q_{\mathrm{h}}-Q_{\mathrm{gap}}+I^2R_{\mathrm{e,Cu}}+I^2R_{\mathrm{e,sol}}+2I^2\frac{R_{\mathrm{e,c1}}+R_{\mathrm{e,c2}}}{A_{\mathrm{TE}}}\end{aligned} \tag{40}$$

where Q_{C} is the net heat absorption at the sharp end of the TEC device, and Q_{H} is the net heat rejection at the hot end of the TEC device. T_{C} and T_{H} are the temperatures of the cold and hot ends of the TEC device, respectively. $R_{\mathrm{k,c1}}$ is the thermal contact resistance of the TE element-solder interface; $R_{\mathrm{k,c2}}$ is the thermal contact resistance of the Cu-solder interface; $R_{\mathrm{e,Cu}}$ is the electrical resistance of copper connector; $R_{\mathrm{e,sol}}$ is the electrical resistance of solder; $R_{\mathrm{e,c1}}$ is the electrical resistance of the TE element-solder interface; $R_{\mathrm{e,c2}}$ is the electrical resistance of the Cu-solder interface.

In practical application, a heat load is typically connected to the cold end of the TEC, and a heat sink is placed at the hot end of the TEC to dissipate the pumped heat into the environment. It is assumed that the electrical and thermal properties of the thermal interface material (TIM) are sufficiently good that the contact resistances can be ignored. The net heat absorption/rejection at the cold/hot end of the TEC device also can be expressed as:

$$Q_{\mathrm{C}}=\frac{T_{\mathrm{load}}-T_{\mathrm{C}}}{R_{\mathrm{k,TIM}}+R_{\mathrm{k,load}}} \tag{41}$$

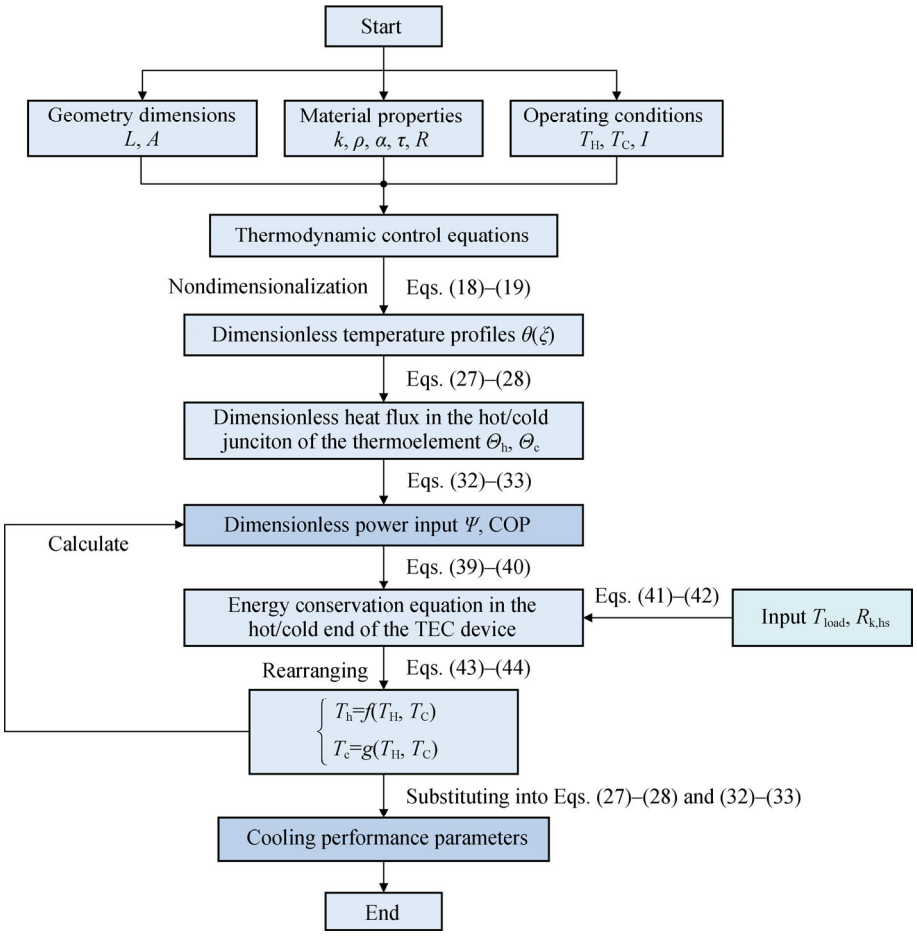

Fig. 2 The calculation flow chart for the mathematical model

$$Q_{\mathrm{H}}=\frac{T_{\mathrm{H}}-T_{\mathrm{a}}}{R_{\mathrm{k,TIM}}+R_{\mathrm{k,hs}}} \tag{42}$$

where T_{load} represents the temperature of the heat load; T_{a} represents the ambient temperature. $R_{\mathrm{k,TIM}}$ represents the thermal resistance of TIM; $R_{\mathrm{k,load}}$ represents the thermal resistance of heat load; $R_{\mathrm{k,hs}}$ represents the thermal resistance of heat sink.

Thus, Eqs. (39) and (40) can be given by:

$$\frac{T_{\mathrm{load}}-T_{\mathrm{c}}}{R_{\mathrm{k,sub}}+\frac{R_{\mathrm{k,c2}}}{A_{\mathrm{Cu}}}+R_{\mathrm{k,Cu}}+R_{\mathrm{k,sol}}+\frac{R_{\mathrm{k,c1}}}{2A_{\mathrm{TE}}}+R_{\mathrm{k,TIM}}+R_{\mathrm{k,load}}}=Q_{\mathrm{c}}-Q_{\mathrm{gap}}-I^2R_{\mathrm{e,Cu}}-I^2R_{\mathrm{e,sol}}-2I^2\frac{R_{\mathrm{e,c1}}+R_{\mathrm{e,c2}}}{A_{\mathrm{TE}}} \tag{43}$$

$$\frac{T_{\mathrm{h}}-T_{\mathrm{a}}}{R_{\mathrm{k,sub}}+\frac{R_{\mathrm{k,c2}}}{A_{\mathrm{Cu}}}+R_{\mathrm{k,Cu}}+R_{\mathrm{k,sol}}+\frac{R_{\mathrm{k,c1}}}{2A_{\mathrm{TE}}}+R_{\mathrm{k,TIM}}+R_{\mathrm{k,hs}}}=Q_{\mathrm{h}}-Q_{\mathrm{gap}}+I^2R_{\mathrm{e,Cu}}+I^2R_{\mathrm{e,sol}}+2I^2\frac{R_{\mathrm{e,c1}}+R_{\mathrm{e,c2}}}{A_{\mathrm{TE}}} \tag{44}$$

Rearranging Eqs. (43) and (44) into the following form:

$$\begin{cases}T_{\mathrm{h}}=f\left(T_{\mathrm{H}},T_{\mathrm{C}}\right)\\ T_{\mathrm{c}}=g\left(T_{\mathrm{H}},T_{\mathrm{C}}\right)\end{cases} \tag{45}$$

Substituting Eq. (45) into Eqs. (27)–(28) and (32)–(33), cooling performance parameters thus can be derived.

3. Experimental Validation

Experiments have been performed to validate the accuracy of the analytical model. The TEC test fixture and experimental setup are shown in Fig. 3. The commercial TEC module 9501/031/040B (15.1×15.1×3.18 mm^3, 31 pairs of thermocouples) fabricated by Ferrotec Corporation and 1MD10-049-20 (12×12×3.1 mm^3, 49 pairs of thermocouples) produced by RMT Ltd were employed in the validation process. The TECs were powered by lab direct current (DC) power supply. The heat load was represented by a Kapton foil heater (Thorlabs, HT10K) that was connected with the cold side of the TEC module. A temperature controller (Thorlabs, TC200) was used to control the heater temperature during the experiments. The hot side of the TEC was connected to two aluminum blocks with dimensions of 40×40×30 mm^3. Four K-type thermocouples (5TC-TT-K-30-36, OMEGA Engineering) with an error of 0.75% were used to measure the temperatures at different locations of the aluminum blocks. The distance between the temperature measurement points was 20 mm. A data acquisition (DAQ) from National Instruments Inc, NI TB-9212 (with an accuracy of 0.29°C), was used to collect the temperatures recorded by the thermocouples. Then the temperature data were transmitted into the computer for storing and processing. A copper heat exchanger was attached to the lower end of the aluminum blocks to maintain a fixed temperature under the PID-controlled water cooling system (with an accuracy of 0.05°C). The use of silicone oil-based thermal joint compound (Wakefield-Vette, 120-8) between different materials provided efficient thermal bonding. At the same time, bolts and nuts were utilized to apply sufficient pressure to reduce the contact resistance between all interfaces.

Fig. 4 shows the comparisons between the analytical results with the experimental results under fixed temperatures at both the cold and hot ends of the TEC devices. It can be seen that for two different sized devices, the analytical results agree well with the experimental results. The deviation between the two results is mainly caused by material parameters, measurement errors, and heat losses. Overall, the maximum error is within 5%, thus validating the analytical model.

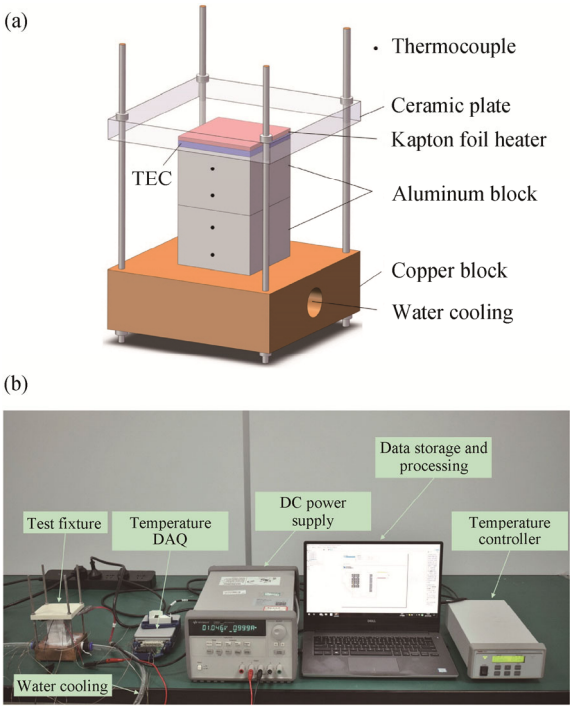

Fig. 3 Scheme of (a) TEC test fixture and (b) experimental setup

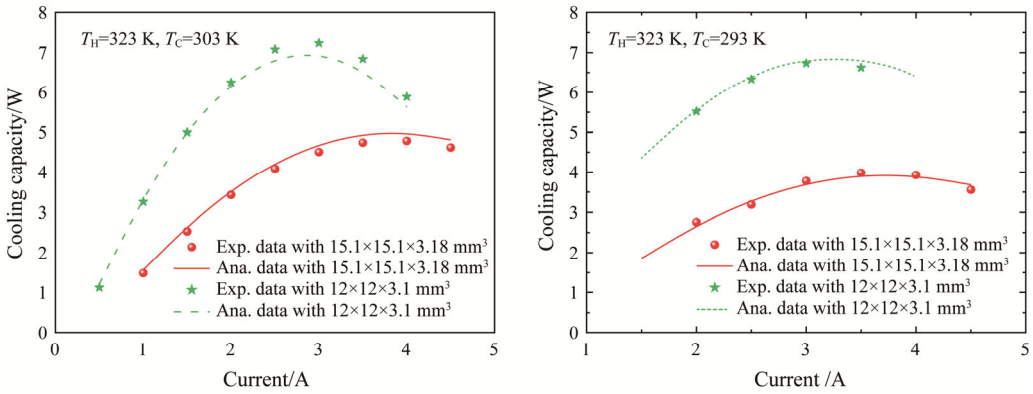

(a) ΔT=20 K (b) ΔT=30 K

Fig. 4 Comparisons between the analytical results and the experimental results: (a) ΔT=20 K and (b) ΔT=30 K

Table 1 Primary parameters of the TEC devices

Parameter	TEC module 1	TEC module 2
Dimensions of the TEC/mm^3	15.1×15.1×3.18	12×12×3.1
Pairs of P, N-type legs	n=31	n=49
Leg length/mm	L_N=L_P=1.48	L_N=L_P=1.9
Leg cross-sectional area/mm^2	A_N=A_P=1.15×1.15	A_N=A_P=1×1
Thermal contact resistance of the TE element-solder interface/K·m^2·W^{-1}	$R_{k,c1}$=6.25×10^{-6} [16]	$R_{k,c1}$=6.25×10^{-6} [16]
Thermal contact resistance of the Cu-solder interface/ K·m^2·W^{-1}	$R_{k,c2}$=4.16×10^{-7} [16]	$R_{k,c2}$=4.16×10^{-7} [16]
Electrical resistivity of copper connector/Ω·m	ρ_{Cu}=1.8×10^{-7}	ρ_{Cu}=1.8×10^{-7}
Electrical resistivity of solder/ Ω·m	ρ_{sol}=1.45×10^{-7}	ρ_{sol}=1.45×10^{-7}
Electrical resistance of the TE element-solder interface (Ω·m^2)	$R_{e,c1}$=7×10^{-11} [16]	$R_{e,c1}$=7×10^{-11} [16]
Electrical resistance of the Cu-solder interface/Ω·m^2	$R_{e,c2}$=3×10^{-12} [16]	$R_{e,c2}$=3×10^{-12} [16]
Gap thermal conductivity/ W·m^{-1}·K^{-1}	0.02	0.02
Thermoelement thermal conductivity/W·m^{-1}·K^{-1}	k_N=0.206+0.005×T–6.960×10^{-6}×T^2 [6] k_P=–0.966+0.011×T–1.378×10^{-5}×T^2 [6]	k_N=5.873–0.026×T+3.946×T^2 [32] k_P=4.187–0.016×T+2.349×T^2 [32]
Thermoelement electrical resistivity/Ω·m	ρ_N=1.298×10^{-5}–3.279×10^{-8}×T+7.712×10^{-11}×T^2 [6] ρ_P=–1.494×10^{-5}+9.487×10^{-8}×T–4.746×10^{-11}×T^2 [6]	ρ_N=–2.041×10^{-6}+3.692×10^{-8}×T+1.155×10^{-11}×T^2 [32] ρ_P=–2.356×10^{-7}+9.045×10^{-9}×T+7.662×10^{-11}×T^2 [32]
Thermoelement Seebeck coefficient/V·K^{-1}	α_N=5.471×10^{-5}–1.059×10^{-6}×T+1.145×10^{-9}×T^2 [6] α_P=–3.027×10^{-4}+2.644×10^{-6}×T–3.348×10^{-9}×T^2 [6]	α_N=–4.967×10^{-5}–8.27×10^{-7}×T+1.008×10^{-9}×T^2 [32] α_P=–4.37×10^{-5}+1.272×10^{-6}×T–1.516×10^{-9}×T^2 [32]

4. Results and Discussion

A new one-dimensional thermodynamic model to evaluate the device-level performance of the thermoelectric cooler subjected to the influences of the Thomson effect, contact resistance, gap heat leakage, heat load, and heat sink has been formulated. In the present study, the commonly used bismuth telluride (Bi_2Te_3) was selected. The properties of Bi_2Te_3 were temperature-dependent within its operation temperature range, including the Seebeck coefficient, thermal conductivity, and electrical resistivity. The primary parameters of the TEC device in calculations were given in Table 1. It was assumed that the cold-end temperature of the TEC device was maintained at 303 K and the hot-end temperature was kept at 323 K. This assumption was very common and can be easily achieved in the area of thermal control for engineering applications. The thermal resistance of TIM was set to 0.05 K·W^{-1}. The thermal resistance of the heat load was assumed to be 0.02 K·W^{-1}.

4.1 The influence of Thomson coefficient

The Thomson effect belonged to the secondary effect, which was given by an electric current flowed in a homogeneous conductor where there was a temperature gradient. The Thomson coefficients can be conveniently obtained for the given thermoelectric materials according to Eq. (7). To analyze the influence of the Thomson effect on the TEC device performance, some typical values were selected arbitrarily for the case study, as shown in Fig. 5 and Table 2. At first, the cooling capacity was obviously increased with the enhancement of the current. However, due to the response of accumulated Joule heat, the cooling capacity began to decrease when the current reached the optimal value. From Case 1 to Case 6, it can be seen that the optimal current of the cooling capacity was increased with the raising Thomson coefficient, whereas the optimal current of the COP was almost unchanged. It was because the hot-end heat flow increased more significantly than the cold-end heat flow with respect to the current, referred to Eqs. (27) and (28). This also meant that the power consumption increased faster than cooling capacity. As a result, the influence of the Thomson effect on cooling capacity continued to expand with increasing current, while the effect on COP hardly changed with current.

In addition, a positive Thomson coefficient for P-type thermoelectric legs and a negative Thomson coefficient for N-type thermoelectric legs can help TEC achieve better performance. At the same current, the higher the absolute value of the Thomson coefficient of the two legs, the stronger the performance improvement. This was because the P-type leg carried free holes whose temperature gradient direction was the same as the direction of the applied current. A positive Thomson coefficient would form a Thomson electromotive force in the thermoelectric circuit that was in the same direction as that of the applied current. In this case, the Thomson electromotive force would give rise to the current within the leg from cold to hot regions. Conversely, N-type legs carried predominantly free electrons moving to the opposite direction of the applied current. Thus, a negative Thomson coefficient was such as to produce a favorable Thomson electromotive force, resulting in a positive Thomson effect. In practice, the Thomson coefficient can be controlled through the introduction of impurities (doping), which provided a direct method for optimizing thermoelectric performance.

4.2 The influence of contact resistance

In an actual thermoelectric device, thermoelectric legs were soldered or welded to the conductive connectors through bonding layers. Contact resistance generated at the interface of the contact layer was thus introduced into the thermoelectric circuit, which would no doubt deteriorate the TEC performance. Fig. 6 depicts the effect of contact resistance on the junction temperatures by comparing four cases consisting of different resistance values. The settings for the cases are shown in Table 3. From the figure, it seems that the effect of contact resistance on the TEC performance was almost negligible. However, the cooling capacity curves of Cases 9 and 10 were a little higher than other cases when the current was large. Thus, the thermal contact resistance had a slightly higher impact on performance than the electrical contact resistance. On the other hand, the thermal contact

Table 2 Cases to study the effect of the Thomson coefficient

Case	τ_P/V·K^{-1}	τ_N/V·K^{-1}	τ_P–τ_N/V·K^{-1}
Case 1	-3×10^{-4}	3×10^{-4}	-6×10^{-4}
Case 2	-2×10^{-4}	2×10^{-4}	-4×10^{-4}
Case 3	-1×10^{-4}	1×10^{-4}	-2×10^{-4}
Case 4	1×10^{-4}	-1×10^{-4}	2×10^{-4}
Case 5	2×10^{-4}	-2×10^{-4}	4×10^{-4}
Case 6	3×10^{-4}	-3×10^{-4}	6×10^{-4}

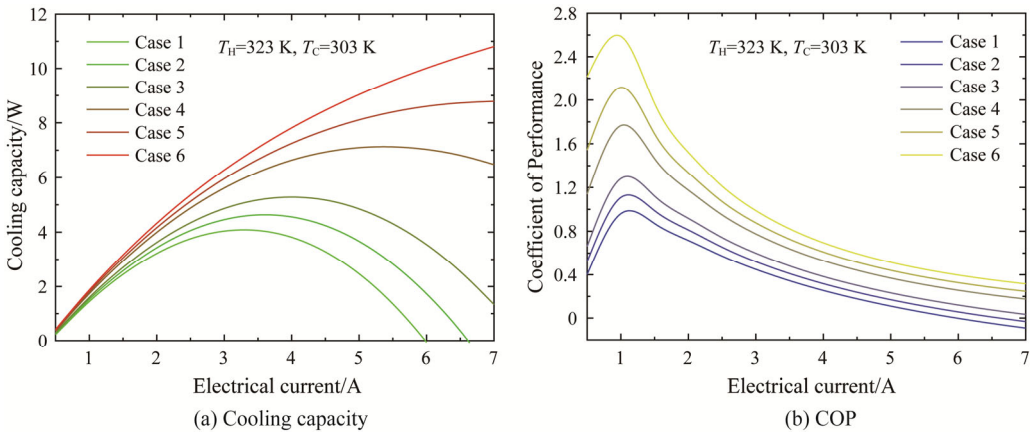

(a) Cooling capacity (b) COP

Fig. 5 The influence of the Thomson effect on the cooling performance of the TEC device for various applied current: (a) cooling capacity and (b) COP

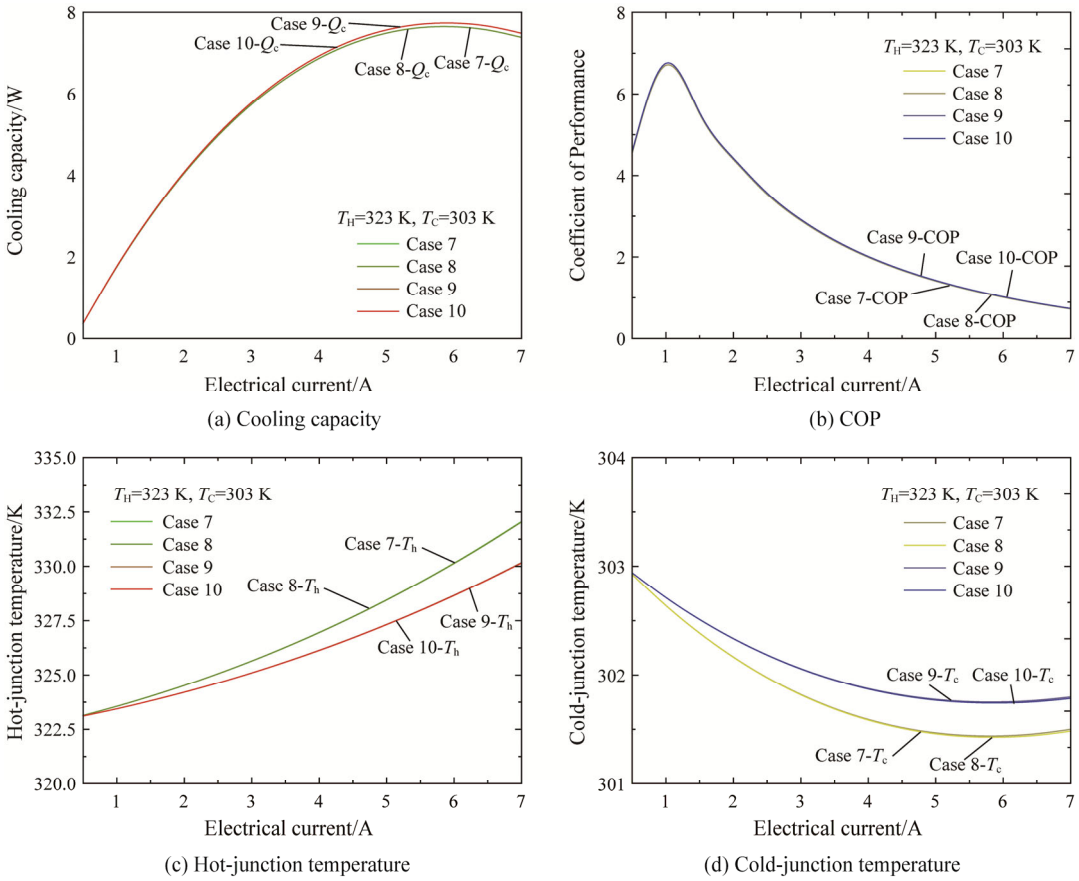

Fig. 6 The influence of the contact resistance on the TEC performance for various applied current: (a) cooling capacity, (b) COP, (c) hot-junction temperature, and (d) cold-junction temperature

Table 3 Cases to study the effect of contact resistance

Case	$R_{k,c1}$/ K·m^2·W^{-1}	$R_{k,c2}$/ K·m^2·W^{-1}	$R_{e,c1}$/Ω·m^2	$R_{e,c2}$/Ω·m^2
Case 7	6.25×10^{-6}	4.16×10^{-7}	7.00×10^{-11}	3.00×10^{-12}
Case 8	6.25×10^{-6}	4.16×10^{-7}	0	0
Case 9	0	0	7.00×10^{-11}	3.00×10^{-12}
Case 10	0	0	0	0

resistance of the hot-junction had the greatest impact, which could make the difference of the hot-junction temperature between cases reach about 2 K, as shown in Fig. 6(c). Therefore, low thermal contact resistance was beneficial to obtain lower hot-junction temperature, which can even reduce 2 K compared with the electrical contact resistance in the case study. As the current continued to increase, the cooling capacity rose rapidly, resulting in a corresponding decrease in the cold-junction temperature of the TEC. When the Joule heat accumulated more and more, the cooling capacity would start to decrease after reaching the peak, which would also cause the cold-junction temperature to rise after hitting the valley point. In general, the cold-junction temperature varied little in different cases. It was worth emphasizing that the boundary conditions in this paper were assumed that the temperatures at both ends of the TEC were fixed, thus reducing the impact of contact resistance on performance. Under actual thermal convection conditions, contact resistance would have a greater impact on TEC performance.

4.3 The influence of heat leakage

Due to the low operating temperature and the small exposed area of the thermoelements, the convection and radiation heat losses were often negligible compared to other factors. In this study, we mainly considered heat leakage through the filling gap. Referring to Eq. (35), the heat leakage of the gap was mainly related to the thermal conductivity of the insulating material and the temperature difference. Therefore, the previous assumption was that the fixed temperatures of both ends of the TEC device were no longer suitable. It was necessary to introduce the thermal load and the heat sink for a comprehensive evaluation. Fig. 7 shows the variation of the cooling capacity with respect to the gap thermal conductivity for various thermal resistances of

the heat sink. The heat leakage had little effect on the cooling performance of the TEC even at large current. But even so, when the thermal conductivity of the filling gap was significantly increased, a reduction in the cooling capacity was still visible. The heat leakage of the gap was a negative factor in the cooling performance of the TEC. In addition, the effect of heat leakage from the filling gap on the performance of the TEC device was higher in the case of smaller thermal resistance of the heat sink. The reason may be that in the case of large current, the negative effect in TEC was mainly caused by the accumulated Joule heat. The influence of heat leakage was negligible compared to the effect of Joule heating. However, when the thermal resistance of the heat sink was small, it was conducive to the dissipation of Joule heat at the hot end of the TEC, which may slightly highlight the effect of heat leakage. Therefore, under the condition that the thermal resistance of the heat sink was small, it was more necessary to use the insulating material with lower thermal conductivity to prevent gap heat leakage. Besides, it should be emphasized that the heat leakage considered in this study was mainly from the gaps between the P- and N-type thermoelements. In practical TEC devices, the gap volumes between different thermoelectric pairs might be even larger. However, since these gaps were difficult to measure, they were not considered in this study.

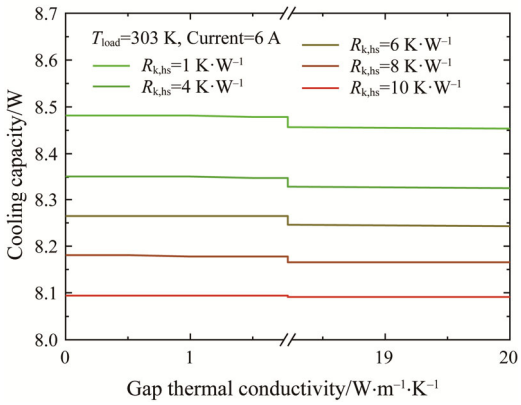

Fig. 7 The influence of the heat leakage on the cooling performance of the TEC device for various thermal resistances of heat sink

4.4 The influence of the thermal resistance of heat sink

Fig. 8 presents the effects of the thermal resistance of heat sink on the cooling performance of the TEC. Under the given heat sink resistance, the cooling capacity was lifted up with the increasing current. When the current reached the optimum value, such as about 6 A in this study, the cooling capacity began to decrease. On the other hand, the COP was continued to decline as the current increased. The thermal resistance of the heat sink represented the corresponding heat dissipation capacity of the hot end of the TEC device. With the increasing thermal resistance of the heat sink, it can be found that the cooling performance of the TEC was significantly reduced, especially the cooling capacity. It was worth noting that when the current reached a larger value, such as 7 A, the cooling capacity curve was steeper and decreased faster. At this time, a large amount of Joule heat was accumulated inside the TEC. If it cannot be effectively eliminated, the cooling performance would be greatly reduced. Therefore, at a large current, the influence of the thermal resistance of heat sink on the cooling performance was even greater. And no matter what the current was, the enhancement of the heat dissipation of the hot end can effectively increase the cooling power. Current high-performance heat exchangers, such as micro-channels, impinging jets, and other heat dissipation methods, can be assembled with the TEC to directly improve the cooling capability of the system.

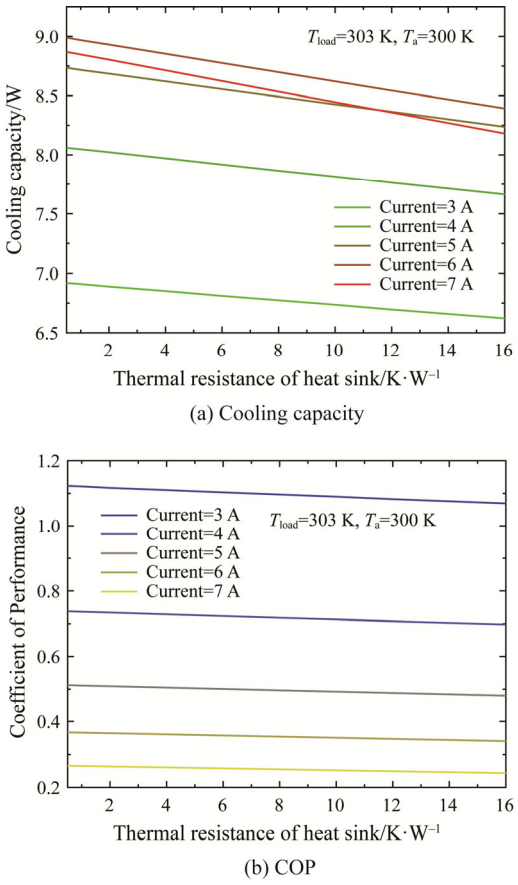

Fig. 8 The influence of the thermal resistance of heat sink on the cooling performance of the TEC device: (a) cooling capacity and (b) COP

4.5 The influence of heat load

Fig. 9 presents the effects of the heat load on the cooling performance for various applied currents. The increase in the heat load temperature indicated that more heat would be transferred to the cold end of the TEC. Clearly, TEC could exert its cooling potential. For example, a heat load of 5 K can increase the cooling capacity by about 4%. However, raising the cooling capacity required a larger drive current to meet the heat pumping requirement of the heat load. Otherwise, the TEC would lose its cooling effect. As shown in Fig. 9(a), under certain thermal load conditions, the cooling performance cannot be calculated for small current conditions. In addition, the COP changed a little and decreased with the increasing current, as shown in Fig. 9(b). The enhanced current would reduce the cooling efficiency of the TEC. At the same time, once the current exceeded the optimum current value, the raising effect to the cooling power would also become smaller and smaller, until the cooling capacity and cooling efficiency of the TEC were reduced to zero. On the other hand, the introduction of heat load would increase the cold end temperature of the TEC device. The cold end could even lose its original cooling effect and exhibit an uneven temperature distribution. Subsequently, large local temperature gradients could create considerable thermal stress, which would severely restrict the reliability of the TEC [33]. Therefore, in order to achieve the functionality of the TEC in actual use, it was necessary to choose an applicable TEC according to the heat load condition and choose the appropriate current conditions.

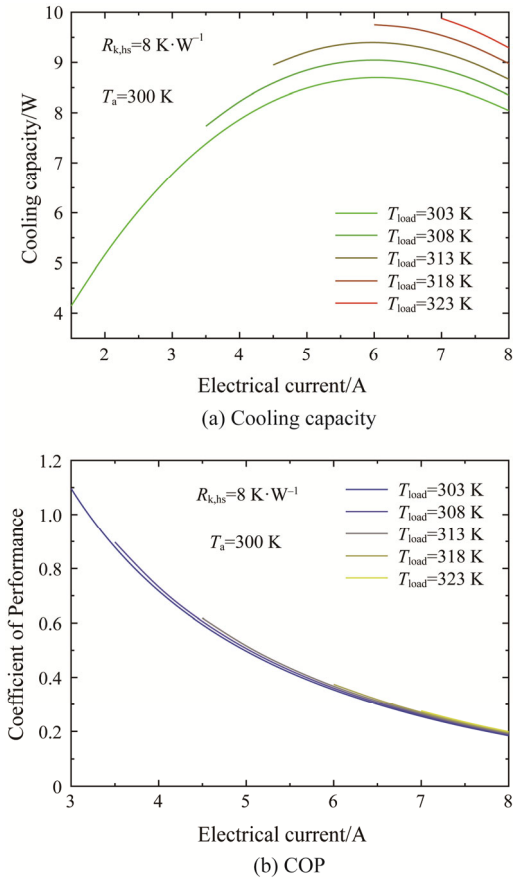

Fig. 9 The influence of the heat load on the cooling performance of the TEC device for various applied currents: (a) cooling capacity and (b) COP

5. Conclusions

In this paper, a one-dimensional thermodynamic model to evaluate the device-level performance of the thermoelectric cooler subjected to the influences of the Thomson effect, contact resistance, gap heat leakage, heat load, and heat sink has been formulated. The model was generalized and simplified by introducing dimensionless parameters. Experimental measurements showed good agreement with analytical results. The sensitivity of the factors that may affect the TEC's cooling performance was analyzed. The main conclusions were as follows:

(1) The influence of the Thomson effect on cooling capacity continued to expand with increasing current, while the effect on COP hardly changed with current. Meanwhile, a positive Thomson coefficient for P-type thermoelectric legs and a negative Thomson coefficient for N-type thermoelectric legs can help TEC achieve better performance. The higher the absolute value of the Thomson coefficient of the two legs, the stronger the performance improvement.

(2) The thermal contact resistance had a slightly higher impact on performance than the electrical contact resistance. Low thermal contact resistance was beneficial to obtain lower hot-junction temperature, which can even reduce 2 K compared with the electrical contact resistance in the case study.

(3) The gap heat leakage was a negative factor affecting the cooling performance. When the thermal resistance of the heat sink was small, the negative effect of heat leakage on performance would be further enlarged. The improvement of the heat dissipation of the hot end can effectively increase the cooling power. At a large current, the influence of the thermal resistance of heat sink on the cooling performance was even more significant.

(4) The enhancement of heat load temperature would increase the cooling power of the TEC device. For example, an increase of 5 K in heat load can increase the cooling capacity by about 4%. However, raising the cooling capacity required continuously increasing the drive current. Otherwise, the TEC would lose its cooling effect. Besides, once the current exceeded the optimum value, the raising impact on the cooling power would

become smaller and smaller until the cooling capacity and the COP were reduced to zero.

Acknowledgments

This study was financially supported by the National Natural Science Foundation of China (NSFC) (Grant No. 52106032), the Science Challenge Program (Grant No. TZ2018003), the National Natural Science Foundation of China (Grant No. 51778511), the Hubei Provincial Natural Science Foundation of China (Grant No. 2018CFA029), and the Key Project of ESI Discipline Development of Wuhan University of Technology (WUT Grant No. 2017001).

References

[1] Majumdar A., Thermoelectric devices: Helping chips to keep their cool. Nature Nanotechnology, 2009, 4(4): 214–215.

[2] Engelmann G., Laumen M., Gottschlich J., et al., Temperature controlled power semiconductor characterization using thermoelectric coolers. IEEE Transactions on Industry Applications, 2018, 54(3): 2598–2605.

[3] Karampasis E., Papanikolaou N., Voglitsis D., et al., Active thermoelectric cooling solutions for airspace applications: the thermicool project. IEEE Access, 2017, 5: 2288–2299.

[4] He R.R., Zhong H.Y., Cai Y., et al., Theoretical and experimental investigations of thermoelectric refrigeration box used for medical service. Procedia Engineering, 2017, 205: 1215–1222.

[5] Shen L., Pu X., Sun Y., et al., A study on thermoelectric technology application in net zero energy buildings. Energy, 2016, 113: 9–24.

[6] Rowe D.M., Thermoelectrics handbook: Macro to nano. CRC press, 2005.

[7] Lee H.S., The Thomson effect and the ideal equation on thermoelectric coolers. Energy, 2013, 56(7): 61–69.

[8] Chen W.H., Liao C.Y., Hung C.I., A numerical study on the performance of miniature thermoelectric cooler affected by Thomson effect. Applied Energy, 2012, 89(1): 464–473.

[9] Lam T.T., Yuan S.W., Fong E., et al., Analytical study of transient performance of thermoelectric coolers considering the Thomson effect. International Journal of Thermal Sciences, 2018, 130: 435–448.

[10] Snyder G. J., Toberer E. S., Khanna R., et al., Improved thermoelectric cooling based on the Thomson effect. Physical Review B, 2012, 86(4): 045202.

[11] Zhou Y., Zhang T., Wang F., et al., Numerical study and optimization of a combined thermoelectric assisted indirect evaporative cooling system. Journal of Thermal Science, 2020, 29(5): 1345–1354.

[12] Min G., Rowe D., Improved model for calculating the coefficient of performance of a Peltier module. Energy Conversion and Management, 2000, 41(2): 163–171.

[13] Jeong E.S., A new approach to optimize thermoelectric cooling modules. Cryogenics, 2014, 59(1): 38–43.

[14] Da Silva L.W., Kaviany M., Micro-thermoelectric cooler: interfacial effects on thermal and electrical transport. International Journal of Heat and Mass Transfer, 2004, 47(10–11): 2417–2435.

[15] Su Y., Lu J., Huang B., Free-standing planar thin-film thermoelectric microrefrigerators and the effects of thermal and electrical contact resistances. International Journal of Heat and Mass Transfer, 2018, 117: 436–446.

[16] Sun D., Shen L., Sun M., et al., An effective method of evaluating the device-level thermophysical properties and performance of micro-thermoelectric coolers. Applied Energy, 2018, 219: 93–104.

[17] Qiu C., Shi W., Comprehensive modeling for optimized design of a thermoelectric cooler with non-constant cross-section: Theoretical considerations. Applied Thermal Engineering, 2020, 176: 115384.

[18] Marchenko O.V., Performance modeling of thermoelectric devices by perturbation method. International Journal of Thermal Sciences, 2018, 129: 334–342.

[19] Wang X., Yu J., Ma M., Optimization of heat sink configuration for thermoelectric cooling system based on entropy generation analysis. International Journal of Heat and Mass Transfer, 2013, 63: 361–365.

[20] Wu Y., Zuo L., Chen J., et al., A model to analyze the device level performance of thermoelectric generator. Energy, 2016, 115: 591–603.

[21] Melnikov A.A., Kostishin V.G., Alenkov V.V., Dimensionless model of a thermoelectric cooling device operating at real heat transfer conditions: maximum cooling capacity mode. Journal of Electronic Materials, 2017, 46(5): 2737–2745.

[22] Zhang H.Y., A general approach in evaluating and optimizing thermoelectric coolers. International Journal of Refrigeration, 2010, 33(6): 1187–1196.

[23] Cai Y., Liu D., Zhao F.Y., et al., Performance analysis and assessment of thermoelectric micro cooler for electronic devices. Energy Conversion and Management, 2016, 124: 203–211.

[24] Pearson M.R., Lents C.E., Dimensionless optimization of thermoelectric cooler performance when integrated within a thermal resistance network. Journal of Heat Transfer, 2016, 138(8): 081301.

[25] Zhou Y., Yu J., Design optimization of thermoelectric cooling systems for applications in electronic devices. International Journal of Refrigeration, 2012, 35(4):

1139–1144.

[26] Lu X., Zhao D., Ma T., et al., Thermal resistance matching for thermoelectric cooling systems. Energy Conversion and Management, 2018, 169: 186–193.

[27] Tan H., Fu H., Yu J., Evaluating optimal cooling temperature of a single-stage thermoelectric cooler using thermodynamic second law. Applied Thermal Engineering, 2017, 123: 845–851.

[28] Gonzalez-Hernandez S., Unification of optimization criteria and energetic analysis of a thermoelectric cooler and heater. Physica A: Statistical Mechanics and its Applications, 2020, 555: 124700.

[29] Guo X., Zhang H., Wang J., et al., A new hybrid system composed of high-temperature proton exchange fuel cell and two-stage thermoelectric generator with Thomson effect: Energy and exergy analyses. Energy, 2020, 195: 117000.

[30] Zhao D., Tan G., A review of thermoelectric cooling: materials, modeling and applications. Applied Thermal Engineering, 2014, 66(1–2): 15–24.

[31] Russel M.K., Ewing D., Ching C.Y., Characterization of a thermoelectric cooler based thermal management system under different operating conditions. Applied Thermal Engineering, 2013, 50(1): 652–659.

[32] Sun D., Shen L., Chen H., et al., Modeling and analysis of the influence of Thomson effect on micro-thermoelectric coolers considering interfacial and size effects. Energy, 2020, 196: 117116.

[33] Gong T., Gao L., Wu Y., et al., Transient thermal stress analysis of a thermoelectric cooler under pulsed thermal loading. Applied Thermal Engineering, 2019, 162: 114240.